Computational methods for mold filling simulation of semi-solid alloys
Hétu, Jean-Francois; Ilinca, Florin

Publisher’s version / Version de l'éditeur:

Modeling of Casting, Welding, and Advanced Solidification Processes-XII, 2009-06-07

Computational Methods for Mold Filling Simulation of Semi-Solid Alloys

Jean-François Hétu[1], Florin Ilinca[1]

[1]National Research Council, 75, de Mortagne, Boucherville,Qc, J4B 6Y4, Canada

Keywords: Dense suspensions; 3D Modeling; Finite Elements; Segregation; Diffusive flux model; Free surface flow

This paper presents a 3D numerical solution algorithm for the simulation of free surface flows of dense suspensions including particle migration phenomena. Segregation of the solid phase in processes such as molding of semi-solid materials affects the rheology of the mixture and therefore filling patterns. Segregation affects also the final properties and characteristics of such molded parts as a non-uniform particles distributions lead to non-uniform mechanical properties. In this work, particle migration is modeled using the diffusion flux model of Phillips et al. [6] and is extended to address 3D mold filling problems. The solution algorithm is validated against flow problems for which experimental and numerical data are available. An ALE formulation is developed and combined to a level-set front capturing method to simulate the piston movement and the evolution of the free surface in molding simulations. The approach is applied to molding problems to study the evolution of particle distributions during molding and in the final molded parts.

INTRODUCTION

The ability to predict segregation of the solid phase in processes such as thixomolding is of special interest since such phenomenon affects the final properties and characteristics of the molded parts. Inhomogeneous particle distribution affects the apparent viscosity and thus the flow during filling. This distribution may also affect the part mechanical properties and determine molding defects.

Various models have been proposed to describe the separation of the solid and fluid constituents in dense suspensions. In mixture models each constituent is considered as a distinct specie of a mixture. The development of the mixture formulation is done by writing the conservation equations for each phase involved in the system. Two sets of momentum, mass and energy conservation equations are therefore written, one set for the liquid phase and one for the solid phase. Interaction between the two phases is taken into account by a momentum exchange term. The system of equations is closed by imposing mass conservation for the entire mixture: the sum of liquid and solid fractions equals the unity. The coupled fluid and solid equations can be solved directly [1, 2]; in such a case the evaluation of the viscosity in the fluid and solid phases separately in needed [1]. To avoid the introduction of a solid phase *viscosity* and for computational efficiency reasons, the mixture model can be further simplified using phase mixture rules. By doing so, the two sets of conservation equations are reduced to one set of conservation equations into which the unknowns are the average mixture velocity, pressure and temperature [3, 4]. The local concentration of the mixture is computed using an additional phase concentration equation. In the case of semi-solid slurries Pineau et al. [4] considered that the mixture behaves as a porous media and used a closure model based on the Darcy equation. This closure model implies that the separation mechanism is mainly driven by pressure gradients; the solid phase will increase in high pressure regions such as stagnation points and before sudden contractions such as the gate. At some point, the Darcy closure model requires the determination of an effective permeability of the slurry as a function of solid fraction. This is done using the Carman-Kozeny equation. Manninen [3] proposes a closure model based on particle drag. In this case the relative velocity between the liquid and solid phases is dependent on the pressure gradient and also on the density difference between the liquid and solid phases. Because of the use of a pressure gradient closure model, mixture models are generally unable to predict the experimentally observed shear-induced particle migration [5].

Particle segregation can also be modelled using dense suspension models in which the segregation mechanism is driven by the shear rate. Conceptually, such models assume that particle-particle collision occurring in the suspension is the main driving force for phase separation. High-shear regions have a higher collision probability than low shear regions, thus based on probabilistic arguments, particles tends to migrate from the high shear flow regions to the low shear flow regions. Phillips et al. [6] introduced the diffusive flux model based on the concept of particle concentration diffusion. The suspension balance model was first introduced by Nott and Brady [7] who introduced the concept of suspension *'temperature'*. Experimental validation of both diffusive flux and suspension balance models is shown in Refs. [8, 9].

The objective of this work is to develop numerical simulation tools for the prediction of particle segregation during molding. A 3D numerical solution algorithm for the simulation of particle migration is presented.

The rest of this communication is organized as follows. First, the gorverning equations describing time-dependent laminar flow along with their boundary and initial conditions are presented. Second, the governing equation describing particle segregation is presented. The ALE formulation used to treat the piston movement in molding problems is also described, followed by the solution algorithm and the finite element approach. Then, the approach is validated for a sudden contraction-expansion flow [10]. Finally, the methodology is applied to predict particle segregation in a more complex molding application.

FLOW AND SEGREGATION EQUATIONS

Flow equations

The flow of incompressible fluids is described by the Navier-Stokes equations:

$$\rho\left(\frac{\partial \mathbf{u}}{\partial t} + \mathbf{u}_c \cdot \nabla \mathbf{u}\right) = -\nabla p + \nabla \cdot (2\eta D_{ij}), \tag{1}$$

$$\nabla \cdot \mathbf{u} = 0, \tag{2}$$

where t, $\mathbf{u}$, p, ρ and η denote time, velocity, pressure, density and viscosity respectively and $D_{ij} = (\partial u_i/\partial x_j + \partial u_j/\partial x_i)/2$ is the strain rate tensor. The convection velocity $\mathbf{u}_c$ is equal to the fluid velocity $\mathbf{u}$ in an Eulerian frame reference, but depends on the mesh velocity $\mathbf{u}_m$ in an ALE formulation: $\mathbf{u}_c = \mathbf{u} - \mathbf{u}_m$. The apparent viscosity of the mixture η is computed as a function of the solid fraction ϕ using a modified Krieger-Dougherty model: $\eta = \eta_r\eta_s$, with $\eta_r = \left(1 - \overline{\phi}\right)^{-1.82}$ where η_s is the viscosity of the suspension (liquid phase), η_r is the relative viscosity of the mixture with respect to that of the suspension, and $\overline{\phi}$ denotes the normalized solid fraction, $\overline{\phi} = \phi/\phi_m$; here ϕ_m denotes the maximum solid fraction ($\phi_m = 0.68$).

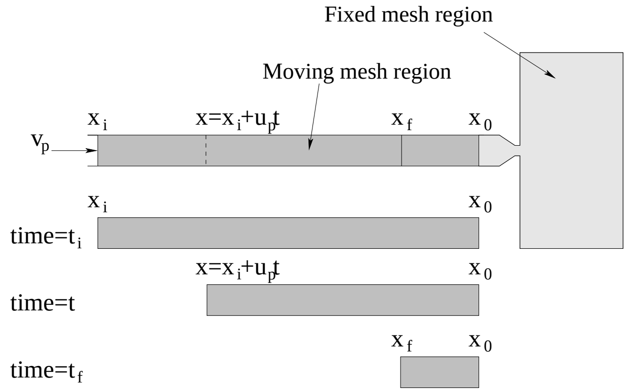

Figure 1: Computational domain change caused by plunger advancement.

Segregation model

In this work we investigate only the case of incompressible mixtures having the same density for the solid particles and the liquid suspension. The segregation of solid particles is modeled by the diffusive flux model of Phillips et al. [6]. The solid fraction is obtained from:

$$\frac{\partial \phi}{\partial t} + \mathbf{u}_c \cdot \nabla \phi = -\nabla \cdot \mathbf{N}, \tag{3}$$

where the diffusive flux $\mathbf{N}$ is given by

$$\mathbf{N} = \mathbf{N}_c + \mathbf{N}_\eta, \quad \text{with} \quad \mathbf{N}_c = -a^2 \phi K_c \nabla \left(\dot{\gamma}\phi\right), \quad \text{and} \quad \mathbf{N}_\eta = -a^2 \phi^2 \dot{\gamma} K_\eta \nabla \left(\ln \eta\right). \tag{4}$$

$\mathbf{N}_c$ describes the interaction caused by varying collision frequency and $\mathbf{N}_\eta$ describes the interaction caused by spatially varying viscosity. In the above equations a represents the radius of solid particles in the suspension, $\dot{\gamma} = \sqrt{2D_{ij}D_{ij}}$ is the shear rate, and K_c, K_η are model constants ($K_c = 0.41$, $K_\eta = 0.62$).

Mold filling simulation

For mold filling applications in addition to solving for the flow equations we have to track in time the position of the interface between the filling material and the air/void inside the cavity. Front tracking is done using a level-set method [11]. For this, a smooth distance function $F(x,t)$ is introduced such that a pre-determined value, F_c, represents the position of the interface. A value larger than F_c indicates a filled region, whereas in empty regions the front tracking function is smaller than F_c. The front tracking function is transported using the velocity field provided by the solution of the momentum-continuity equations:

$$\frac{\partial F}{\partial t} + \mathbf{u}_c \cdot \nabla F = 0. \tag{5}$$

Variable domain modeling

The ultimate goal of this research is the simulation of the segregation occurring in molding processes during which the material is pushed into the mold cavity by means of a plunger/screw. To represent the flow behavior and segregation mechanism we need to model the plunger advancement and hence consider changes in the computational domain. This is done by means of an Arbitrary Lagrangian-Eulerian formulation (ALE) with the geometrical change given by simple relationships depending on the plunger speed. The change of the computational domain in time is illustrated in Figure 1. The portion of the computational domain located between the initial plunger position $x = x_i$ and a fixed location $x = x_0$ (shown in darker gray scale in Figure 1) changes in time to account for the actual plunger position. At any given time t, this volume will be considered between the actual plunger location $x = x_i + u_p t$ and the fixed location $x = x_0$. The mesh is therefore deformed in time as given by the change of variables $x \rightarrow x^*$:

$$x^*(t) = \begin{cases} x + \dfrac{x_0 - x}{x_0 - x_i} u_p t & \text{for } \ x \in [x_i, x_0] \\ x & \text{for } \ x \notin [x_i, x_0] \end{cases} \tag{6}$$

where u_p is the plunger velocity, x is the coordinate of a mesh point in the initial undeformed mesh (at $t = 0$) and x^* is the coordinate of the respective point in the deformed mesh. At the end of the filling ($t = t_f$) the plunger will be located at $x = x_f$ where $x_f = x_i + u_p t_f$. As the mesh deforms, the ALE formulation of the conservation equations has to take into account for the mesh velocity given by:

$$u_m = \frac{\mathrm{d}x^*}{\mathrm{d}t} = \begin{cases} \dfrac{x_0 - x}{x_0 - x_i} u_p & \text{for } \ x \in [x_i, x_0] \\ 0 & \text{for } \ x \notin [x_i, x_0] \end{cases} \tag{7}$$

Boundary conditions

The problem definition is completed by imposing boundary conditions. For the injection molding application, no-slip boundary conditions are imposed on the cavity walls filled by the suspension, while on the unfilled part, a free boundary condition allows for the formation of the typical fountain flow. The solid fraction is set to an initial value and then a zero solid fraction flux is imposed on the boundary. This will ensure that the total particle concentration remains constant inside the computational domain.

FINITE ELEMENT SOLUTION

Model equations are discretized in time using a first order implicit Euler scheme. Linear continuous shape functions are used for all variables. At each time step, the global system of equations is solved in a partly segregated manner. See [11] for further information.

Flow equations

The Navier-Stokes equations (1) and (2) are solved using a Galerkin Least-Squares (GLS) method. This method contains an additional pressure stabilization term compared with the standard Galerkin method. In such a way, the use of linear elements for both the velocity and pressure is permitted. The GLS variational formulation of the momentum-continuity equations is:

$$\begin{aligned} &\int_\Omega \rho \left(\frac{\partial \mathbf{u}}{\partial t} + \mathbf{u}_c \cdot \nabla \mathbf{u} \right) \mathbf{v} d\Omega + \int_\Omega 2\eta D_{ij}(\mathbf{u}) : D_{ij}(\mathbf{v}) d\Omega - \int_\Omega p \nabla \cdot \mathbf{v} d\Omega + \int_\Omega \nabla \cdot \mathbf{u} q d\Omega \\ &+ \sum_K \int_{\Omega_K} \left\{ \rho \left(\frac{\partial \mathbf{u}}{\partial t} + \mathbf{u}_c \cdot \nabla \mathbf{u} \right) + \nabla p - \nabla \cdot [2\eta D_{ij}(\mathbf{u})] \right\} \cdot \tau_u \left\{ \rho \mathbf{u}_c \cdot \nabla \mathbf{v} + \nabla q \right\} d\Omega_K = 0 \end{aligned} \tag{8}$$

where $\mathbf{v}$ and q are the velocity and pressure test functions respectively. The stabilization parameter τ_u is defined as: $\tau_u = \left[\left(\frac{2\rho}{\Delta t}\right)^2 + \left(\frac{2\rho|\mathbf{u}_c|}{h_K}\right)^2 + \left(\frac{4\eta}{m_k h_K^2}\right)^2\right]^{-1/2}$. Here Δt is the time step, h_K is the size of the element K and m_k is a coefficient set to 1/3 for linear elements (see [11]).

Solid fraction equation

The solid fraction equation is solved by a SUPG method. SUPG provides smooth solutions when the convective part of the equation is dominant, as is in the present case. The finite element formulation, once the diffusive flux term is integrated by parts, is as follows:

$$\int_\Omega \left(\frac{\partial \phi}{\partial t} + \mathbf{u}_c \cdot \nabla \phi\right) w \mathrm{d}\Omega - \int_\Omega (\mathbf{N}_c + \mathbf{N}_\eta) \cdot \nabla w \mathrm{d}\Omega$$
$$+ \sum_K \int_{\Omega_K} \left(\frac{\partial \phi}{\partial t} + \mathbf{u}_c \cdot \nabla \phi\right) \tau_\phi \mathbf{u} \cdot \nabla w \mathrm{d}\Omega_K = - \int_{\partial\Omega} (\mathbf{N}_c + \mathbf{N}_\eta) \cdot \hat{\mathbf{n}} w \mathrm{d}\Gamma. \quad (9)$$

Note that by integrating by parts the diffusive flux term $(\mathbf{N}_c + \mathbf{N}_\eta)$, differentiation of the flux terms $\mathbf{N}_c$ and $\mathbf{N}_\eta$ is avoided. However, the derivative of the shear rate is still present in the expression of $\mathbf{N}_c$ along with the derivative of the viscosity in that of $\mathbf{N}_\eta$. Because the velocity field is approximated using piecewise linear elements, the shear rate $\dot{\gamma}$ is constant per element, thus leading to $\nabla\dot{\gamma}$ to be identically zero. Therefore, a L^2 projection, $\dot{\gamma}^*$, of the finite element shear rate into the space of linear continuous interpolation functions is used in the computation of the diffusive fluxes $\mathbf{N}_c$ and $\mathbf{N}_\eta$.

Front tracking equation

The front tracking equation is discretized using an SUPG finite element method. See [11] for further information.

VALIDATION

In this section the solution algorithm is validated on a sudden contraction-expansion flow [10].

Sudden contraction-expansion flow

In this test case the suspension is pushed by a piston from a reservoir pipe into a smaller diameter pipe and then into another larger catch pipe. The flow conditions follow those of the experimental study by Altobelli et al. [10]. The reservoir pipe and the catch pipe have a diameter of $5.08cm$, while the smaller pipe has an inner diameter of $1.27cm$. The smaller diameter pipe is $38cm$ long. Initially $30cm$ of the reservoir pipe, the entire smaller diameter pipe and $4cm$ of the catch pipe were filled. The plunger was displaced at a constant velocity of $0.0625cm/s$, resulting in a mean velocity of $1cm/s$ in the smaller pipe. The solid particles in the suspension were 50% by volume with a mean particle diameter of $675\mu m$.

The numerical solution was obtained using the ALE formulation. The mesh changes with time in both larger diameter pipes, but remains fixed in the smaller diameter pipe. The initial computational mesh and solid fraction and those after the piston moves 2, 4 and respective 6 larger section diameters are shown in Figure 2. The mean solid fraction along the pipe axis is shown in Figure 3. Several observations can be drawn from these results. First, we remark that the solid fraction decreases at the surface of the moving piston. Second, we observe a sharp increase in the solid fraction just prior to the 4:1 contraction ($x = 0cm$). The solid fraction decreases then rapidly and reaches smaller values along the smaller diameter pipe. Third, we remark that at the 1:4 expansion, $x = 38cm$, the solid fraction decreases before the section change and increases on a very small region after the expansion. In the catch pipe, $x > 38cm$, the solid fraction is initially smaller than the mean value of 0.5, but increases towards the end of the pipe.

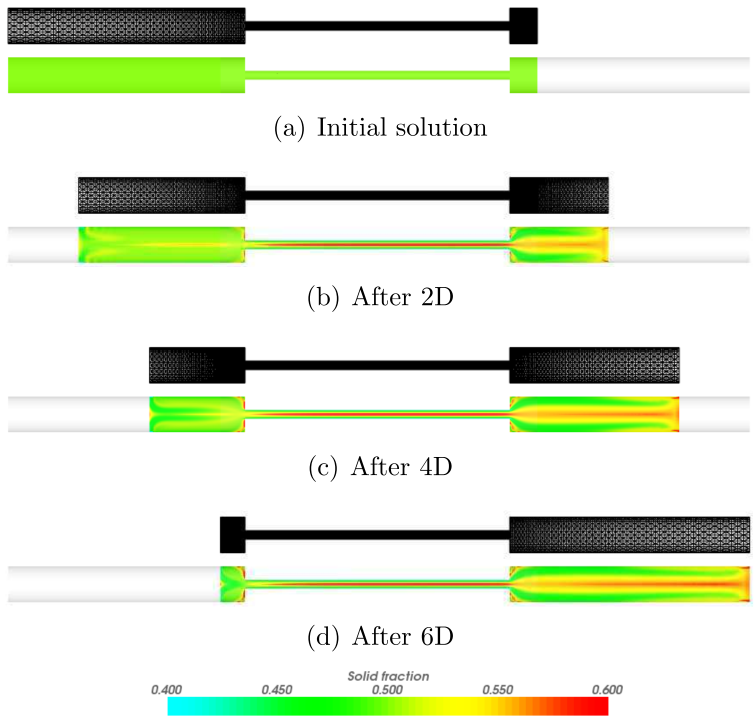

(a) Initial solution

(b) After 2D

(c) After 4D

(d) After 6D

Figure 2: Contraction-expansion flow: Computational mesh and distribution of solid fraction for various piston displacements.

Figure 3(b) shows the solid fraction distribution in radial direction at various locations along the smaller diameter pipe together with the experimental data of Altobelli et al. [10]. Results are plotted for $x/L = 0.1$, 0.5 and 0.95, where L denotes the length of the smaller diameter pipe and x is the coordinate along the pipe measured in the sense of the flow (from the contraction, $x = 0$, towards the expansion, $x = L$). The results indicate that the solid fraction is larger near the axis of the pipe and decreases close to the pipe wall. We remark also that the segregation is more pronounced at $x/L = 0.5$ and 0.95 than at the entry of the smaller diameter pipe. These observations agree well with the experimental findings of Altobelli et al. [10].

MOLD FILLING APPLICATION

In this application the ALE formulation is used to solve the injection molding of a rectangular plate. The plate is $8cm$ by $6cm$ and has $4mm$ in thickness. The filling piston has a radius of $1cm$ and his displacement is $13.2cm$. Filling of the plate is made through a circular gate with a radius of $2mm$. The suspension contains particles of $100\mu m$ in diameter and the initial solid fraction is uniform at 50%. Complete filling of the plate takes $10s$. The filling pattern and the solid fraction distribution is shown in Figure 4 after $1.7s$, $4s$, $7.2s$ and respectively $10s$. The figure shows a cut along the symmetry plane parallel to the longest side of the

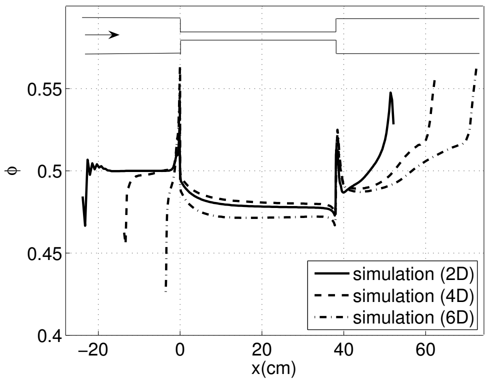

(a) Along pipe axis

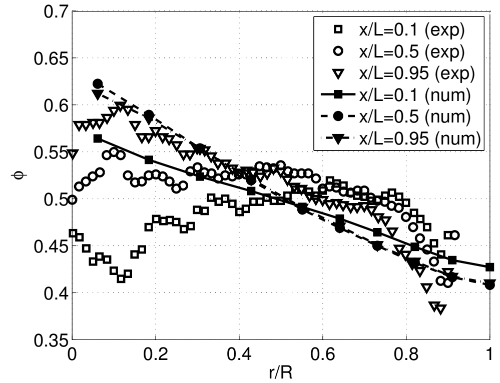

(b) Radial direction

Figure 3: Contraction-expansion flow: simulation results compared with experiments.

plate in order to see the solid fraction distribution inside the part. The images show both the complete domain, where the displacement of the piston during the filling is clearly seen, and details of the flow inside the plate. Segregation of solid particles is apparent inside the pipe. This causes the material to enter the gate with a non-uniform solid fraction. Additional segregation is observed inside the gate where shear rates are highest. Finally, the molded part has higher solid fraction in the mid-plane and on the outside boundaries of the plate and lower solid fraction on the upper and lower surfaces.

CONCLUSION

In this paper, a three-dimensional finite element algorithm is presented to model and simulate free surface flows of dense suspensions. The segregation of solid particles is described by a diffusive flux model. Validation cases show a good agreement with experimental data and previously published numerical predictions. The application to injection molding problems is done by using an ALE formulation. Application to the mold filling of a rectangular plate shows the ability to use this method to the solution of powder injection molding.

References

[1] T. Barrière, J. C. Gelin, and B. Liu, "Improving mould design and injection parameters in metal injection moulding by accurate 3D finite element simulation," *J. of Material Process. Techn., A*, vol. 125-126, pp. 518–524, 2002.

[2] J. Petera, and M. Kotynia, "The finite element model of non-isothermal semi-solid fluid flow," *J. Heat Mass Transfer*, vol. 47, pp. 1483–1498, 2004.

[3] M. Manninen and V. Taivassalo, "On the mixture model for multiphase flow," *VTT Publications, Finland*, vol. 288, 1996.

[4] F. Pineau, F. Ilinca, and J.-F. Hétu, "A mixture approach for semisolid metal mold filling simulations," Proc. MCWASP 2006, *TMS*, 2006.

[5] D. Leighton, and A. Acrivos, "The shear-induced migration of particles in concentrated suspensions," *J. Fluid Mech.*, vol 181, pp. 415–439, 1987.

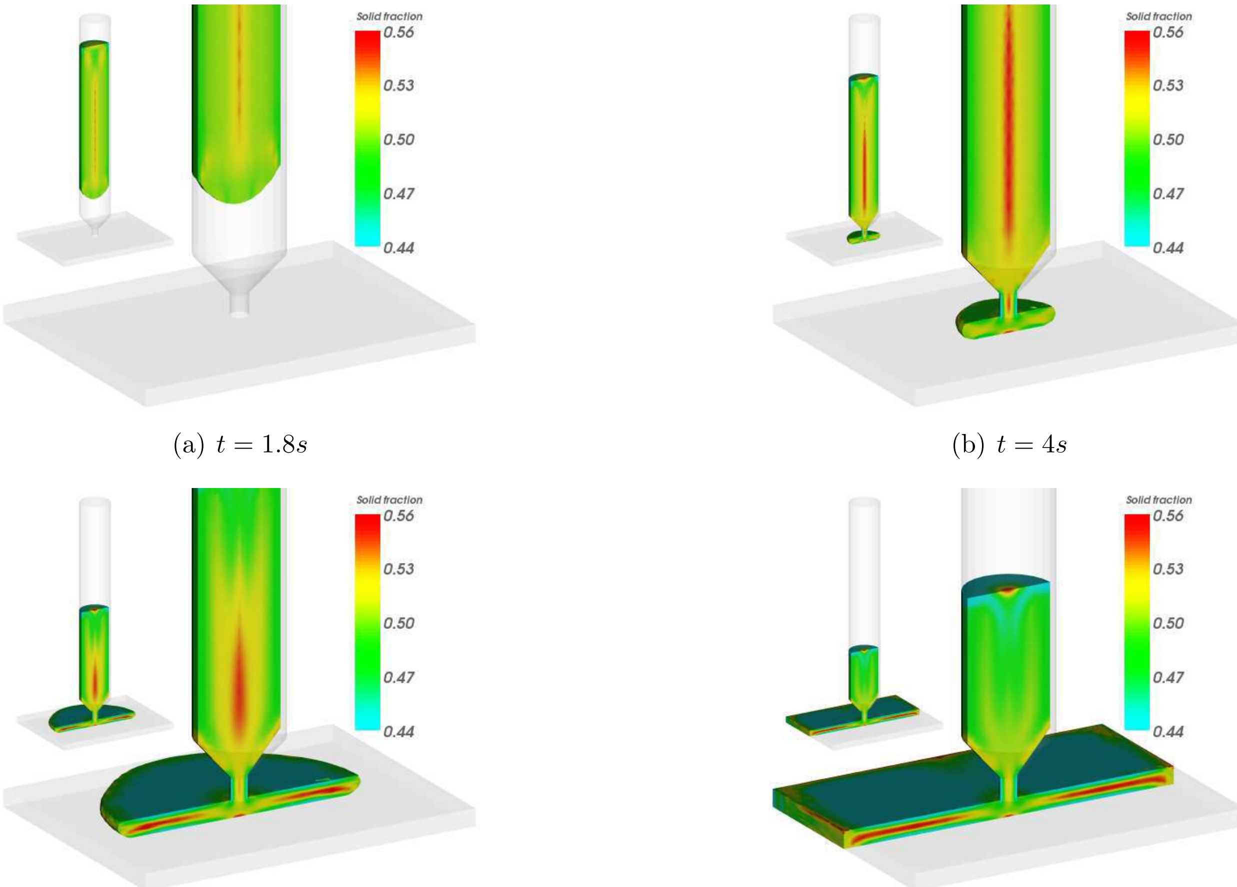

(a) $t = 1.8s$ (b) $t = 4s$

(c) $t = 7.2s$ (d) $t = 10s$

Figure 4: Distribution of solid fraction for the injection of a plate.

[6] R.J. Phillips, R.C. Armstrong, R.A. Brown, A.L. Graham, and J.R. Abott, "A constitutive equation for concentrated suspensions that accounts for shear-induced particle migration," *Physics of Fluids, A*, vol. 4, pp. 30–40, 1992.

[7] P. R. Nott, and J.F. Brady, "Pressure driven flow of suspensions: simulation and theory," *J. Fluid Mech.*, vol. 275, pp. 157-199, 1994.

[8] M.K. Lyon, and L.G. Leal, "An experimental study of the motion of concentrated suspensions in two-dimensional channel flow. Part 1. Monodisperse systems," *J. Fluid Mech.*, vol. 363, pp. 25-56, 1998.

[9] N.C. Shapley, R.A. Brown, and R.C. Armstrong, "Evaluation of particle migration models based on laser Doppler velocimetry measurements in concentrated suspensions," *J. Rheol.*, vol. 48(2), pp. 255–279, 2004.

[10] S.A. Altobelli, E. Fukushima, and L.A. Mondy, "Nuclear magnetic resonance imaging of particle migration in suspensions undergoing extrusion," *J. Rheol.*, vol. 41(5), pp. 1105–1115, 1997.

[11] F. Ilinca, and J.-F. Hétu, "Three-Dimensional free surface flow simulation of segregating dense suspension," *Int. J. Num. Methods Fluids.*, vol. 58, pp. 451–472, 2008.